Applied Mathematics, 2025, 16(9), 657-667
https://www.scirp.org/journal/am
ISSN Online: 2152-7393
ISSN Print: 2152-7385

# Extreme Value Statistics Suggest Enhanced Fuel Implosion Efficiency Using Seven Sequential Sets of 26 Lasers Compared to Simultaneous Firing of 192 Lasers at NIF

**Motohisa Osaka**

Department of Basic Science, Nippon Veterinary and Life Science University, Tokyo, Japan
Email: osaka@nms.ac.jp

**How to cite this paper:** Osaka, M. (2025) Extreme Value Statistics Suggest Enhanced Fuel Implosion Efficiency Using Seven Sequential Sets of 26 Lasers Compared to Simultaneous Firing of 192 Lasers at NIF. *Applied Mathematics*, **16**, 657-667.
https://doi.org/10.4236/am.2025.169036

**Received:** August 13, 2025
**Accepted:** September 2, 2025
**Published:** September 5, 2025



## Abstract

Power generation from hydrogen fusion is the ultimate benefit for humanity. The achievement by National Ignition Facility (NIF) in 2022 of producing energy exceeding the input energy using lasers was a great step forward. However, since the laser was applied indirectly, only 14.2% of its total thermal output was delivered to the fuel. Therefore, the purpose of this study is to identify improvements that would enable the total laser output to more efficiently induce nuclear fusion. One such improvement is to irradiate the fuel uniformly with the lasers so as to avoid imbalance in implosion. In this study, we define the range in implosion velocity as an indicator of imbalance, assuming it to be the difference between the maximum and minimum velocities among the $n$-laser-induced implosion measures. It is then found, based on extreme value statistics commonly used in probability theory, that with 26 lasers the range decreases by 27.6% compared to the 192 lasers used at NIF. A set of 26 laser devices is arranged along a long cylinder, with seven such sets positioned in sequence. A spherical fuel pellet is then allowed to free-fall from the top of the cylinder, and at the moment it passes through each set, the lasers are fired simultaneously. This method enables the fuel to be irradiated directly and continuously. It is estimated that ignition will be achieved if 182 (*i.e.*, 26 × 7) of the 192 lasers used at NIF are arranged around the cylinder.

## Keywords

Laser Fusion, National Ignition Facility, Inertial Confinement Fusion

## 1. Introduction

In recent years, research aimed at achieving nuclear fusion power generation has been actively conducted [1]-[3]. There are two major approaches: magnetic confinement and inertial confinement. Among the former, the tokamak-type fusion reactor is the most prominent, with over 50 years of accumulated knowledge and massive investments, as exemplified by ITER. In the latter category, the laser fusion reactor is representative. In 2024, the author published a paper arguing from a probabilistic perspective that laser fusion is likely to be more energy-efficient than magnetic confinement [4]. In that paper, the author concluded that in magnetic confinement, the extremely strong magnetic fields cause electrons to undergo Larmor motion, which restricts their movement to one dimension and makes it more difficult for them to separate from hydrogen protons. This inhibits plasma generation, meaning that excessively strong magnetic fields actually reduce energy efficiency.

On the other hand, in 2022, the National Ignition Facility (NIF) succeeded in producing a burning plasma using a laser fusion experimental reactor [5]. In this report, the thermal output of the laser was 1900 kJ, of which 270 kJ was delivered to the fuel, resulting in 1370 kJ of heat generated by nuclear fusion. While the energy produced by fusion was less than the total laser input, it exceeded the amount of heat delivered to the fuel, making this a groundbreaking result demonstrating the utility of laser fusion. If laser irradiation can achieve symmetry within the cavity where the fuel is placed, implosion efficiency improves. However, in practice, ensuring perfect symmetry proved difficult. In this experiment, 192 laser drivers were used, and the lasers were irradiated onto a cavity containing the fuel. It was estimated that 4% of the fuel underwent fusion. To further enhance implosion, it might seem that increasing the number of laser drivers would be effective. However, doing so may increase asymmetry, which could instead hinder successful implosion. In the NIF report, the probability distribution of the indirectly generated burning plasma (referred to as G-fuel in the paper) was illustrated. Although the report did not provide detailed discussion of this distribution, in our research, we assume a general Weibull distribution, which is extremely useful for understanding various scientific problems and is also highly valuable in extreme value statistics we are dealing with [6]. This allows us to clarify how much asymmetry increases as the number of simultaneous laser irradiations increases when using similar laser drivers as NIF. As a result, we probabilistically conclude that instead of increasing the number of lasers beyond 192, it will be better to increase the energy of each individual laser. In the web news "*Enhanced Yield Capability Proposal Aims to Boost NIF Yield*", a power-upgrade plan for NIF is presented, in which additional laser glass slabs are inserted into the power amplifiers of the existing beamlines. This approach is expected to enhance the laser performance by up to 40%, potentially increasing the current energy from approximately 2.2 MJ to 3 MJ [7].

Currently, a drawback of laser output devices is that they must be cooled after each irradiation before they can be used again. Additionally, in direct laser-fuel irradiation, the energy released from the fuel may rebound toward the devices. To avoid this, NIF irradiated lasers into a cavity containing the fuel. While implosion efficiency increases with symmetrical irradiation within the cavity, maintaining such symmetry remains difficult. Furthermore, at other research facilities, lasers are first reflected off mirrors and then indirectly irradiate the fuel.

A series of major issues remain for laser fusion power generation, including:

How to achieve continuous laser irradiation,

How to ensure symmetrical irradiation inside the cavity without using mirrors, and,

How to create mirrors that can withstand the heat from imploded fuel if mirrors are used.

This study proposes a method to simultaneously address all of these challenges.

To summarize the structure of the paper:

1) The *Introduction* presents the current achievements in the field of laser fusion and outlines the challenges that must be addressed to achieve more efficient fusion.

2) Based on the results from NIF, the probabilistic limitations of increasing the number of laser drivers beyond 192 are examined.

3) Building on the findings from (2), a proposal is made for a more efficient fusion system.

## 2. Effect of Varying the Number of Laser Devices on Implosion Range

In the NIF experimental reactor, 192 laser irradiation devices were used [5]. Since the work done on the fuel—referred to as *G-fuel* in the NIF paper—exhibited a probability distribution, it can be inferred that the effects of these 192 lasers on the fuel varied. Therefore, increasing the number of lasers would likely result in even greater range in their effects on the fuel. Because uniform and symmetrical laser irradiation is essential for efficient fuel ignition, simply increasing the number of laser drivers is presumed to have limitations. In other words, increasing the number of laser devices with the same output as those used in NIF would increase the total heat delivered to the fuel. However, it is anticipated that this would also increase the range in irradiation, making it more difficult to achieve implosion. Therefore, this study aims to probabilistically clarify the relationship between the number of devices and the range.

To that end, the following hypothesis is proposed:

1) The implosion is influenced by the velocity $v$ of the localized explosions that occur when the laser irradiates the fuel.

2) The velocity $v \equiv \sqrt{v_x^2 + v_y^2 + v_z^2}$, where $v_x$, $v_y$, and $v_z$ follow a normal distribution $N\left(0, \sigma^2\right)$.

Under this assumption, the probability density function and cumulative distribution function of the velocity $v$ are

$$f(v) = \frac{1}{\sigma^3}\sqrt{\frac{2}{\pi}} v^2 e^{-v^2/2\sigma^2} \text{ for } v \geq 0. \quad (1)$$

$$F(v) = erf(v) - \frac{1}{\sigma}\sqrt{\frac{2}{\pi}} v e^{-\frac{v^2}{2\sigma^2}}; erf\text{, error function.} \quad (2)$$

This cumulative distribution function can be qualitatively approximated by the velocity in two dimensions, as shown below. By doing so, it becomes analytically possible—and therefore extremely useful—to calculate the range, defined as $\text{range} \equiv v_{192} - v_1$, where $(v_1, v_2, v_3, \cdots, v_{192})$ are the implosion velocities at the 192 irradiation points, sorted from smallest to largest, when 192 laser devices irradiate the fuel. This range is the range used in statistics. Although there are three possible directional combinations, we consider $v \equiv \sqrt{v_x^2 + v_y^2}$ without loss of generality. The probability density function of $v$ is the well-known Rayleigh probability function:

$$r(v) = \frac{1}{\sigma^2} v e^{-v^2/2\sigma^2} \text{ for } v \geq 0. \quad (3)$$

The cumulative distribution function $R(v)$ is

$$R(v) = \int_0^v r(v) \mathrm{d}v = 1 - e^{-v^2/2\sigma^2}. \quad (4)$$

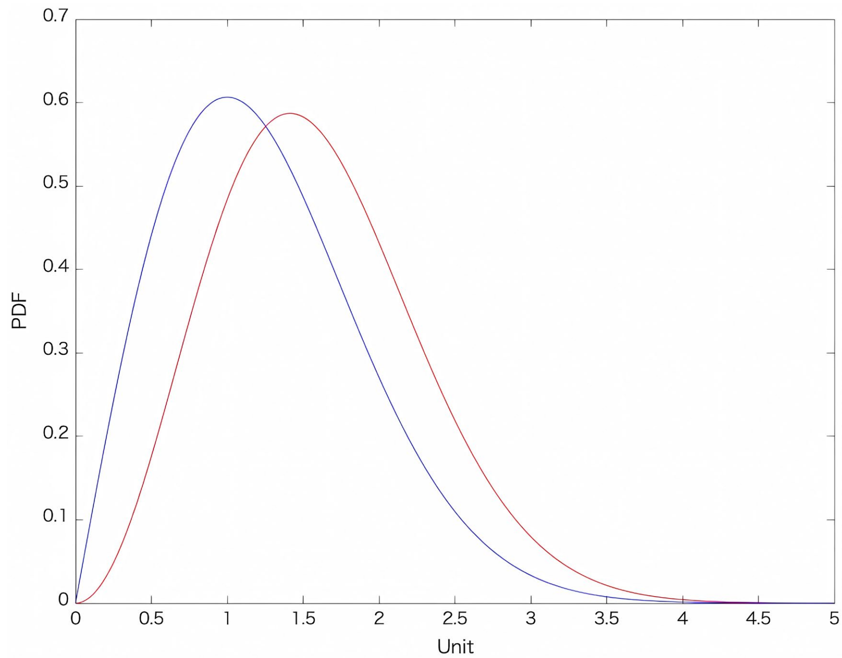


**Figure 1.** Comparison of the probability density functions (PDF) of the implosion velocity in two dimensions and three dimensions: the blue line, the PDF of the two-dimensional implosion velocity, and the red line, the PDF of the three-dimensional implosion velocity. The unit of the ticks on the horizontal axis is the standard deviation, $\sigma$.

When $f(v)$ and $r(v)$ are plotted (**Figure 1**), they both qualitatively exhibit a similar bell-shaped distribution. Therefore, L'Hôpital's rule can be applied, as shown in Equations (13) and (21) below. Although there is a slight difference in the value of $v$ at which the probability density reaches its maximum, the two functions agree closely for $v \geq 3\sigma$. Moreover, $F(v)$ and $R(v)$ are quite similar (**Figure 2**).

Therefore, the following analysis will be conducted using the Rayleigh probability function. By approximating the three-dimensional velocity in two dimensions, the range can be analytically calculated as shown below. The validity of this approximation is discussed in detail in connection with Equations (15), (17), (23), and (25).

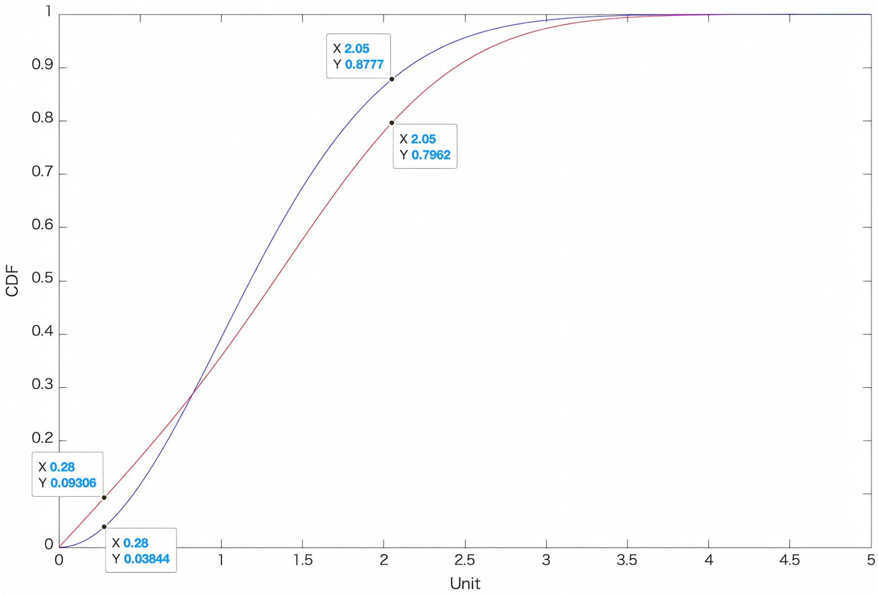


**Figure 2.** Comparison of the cumulative distribution functions (CDF) of the implosion velocity in two dimensions and three dimensions: the blue line, the CDF of the two-dimensional implosion velocity, and the red line, the CDF of the three-dimensional implosion velocity. The unit of the ticks on the horizontal axis is the standard deviation, $\sigma$.

Here we use extreme value statistics [6]. Let the number of laser devices be $n$, and let the set of arbitrary implosion velocities be $(u_1, u_2, u_3, \cdots, u_n)$. When this set is rearranged in ascending order to obtain $(v_1, v_2, v_3, \cdots, v_n)$, the number of possible combinations of the original $(u_1, u_2, u_3, \cdots, u_n)$ is $n!$. Therefore, the joint probability density function of $(v_1, v_2, v_3, \cdots, v_n)$ is

$$g(v_1, v_2, v_3, \cdots, v_n) = n!r(u_1)r(u_2)\cdots r(u_n) = n!r(v_1)r(v_2)\cdots r(v_n).$$

The probability density function of the largest value, $V_n$, can be obtained in terms of $r(v)$ and the cumulative distribution function $R(v)$ as follows:

$$\begin{aligned} g(v_n) &= \int_0^{v_n}\cdots\int_0^{v_3}\int_0^{v_2} n!r(v_1)r(v_2)r(v_3)\cdots r(v_n)\mathrm{d}v_1\mathrm{d}v_2\cdots\mathrm{d}v_{n-1} \\ &= n!r(v_n)\int_0^{v_n}\cdots\int_0^{v_3}\left[\int_0^{v_2} r(v_1)\mathrm{d}v_1\right]\times r(v_2)\cdots r(v_{n-1})\mathrm{d}v_2\cdots\mathrm{d}v_{n-1} \\ &= n!r(v_n)\int_0^{v_n}\cdots\int_0^{v_4}\left[\int_0^{v_3} R(v_2)r(v_2)\mathrm{d}v_2\right]\times r(v_3)\cdots r(v_{n-1})\mathrm{d}v_3\cdots\mathrm{d}v_{n-1} \\ &= n!r(v_n)\int_0^{v_n}\cdots\int_0^{v_5}\left[\int_0^{v_4}\frac{1}{2!}\left[\{R(v_3)\}^2 r(v_3)\right]\mathrm{d}v_3\right]\times r(v_4)\cdots r(v_{n-1})\mathrm{d}v_4\cdots\mathrm{d}v_{n-1} \\ &= n!r(v_n)\int_0^{v_n}\cdots\int_0^{v_6}\left[\int_0^{v_5}\frac{1}{3!}\left[\{R(v_4)\}^3 r(v_4)\right]\mathrm{d}v_4\right]\times r(v_5)\cdots r(v_{n-1})\mathrm{d}v_5\cdots\mathrm{d}v_{n-1}. \end{aligned} \tag{5}$$

Finally, we can derive

$$g(v_n) = n!r(v_n)\frac{\{R(v_n)\}^{n-1}}{(n-1)!} = n\cdot r(v_n)\{R(v_n)\}^{n-1}. \tag{6}$$

Therefore, the cumulative distribution function of $V_n$ becomes

$$G(v_n) = \int_0^{v_n} g(v_n)\mathrm{d}v_n = \{R(v_n)\}^n. \tag{7}$$

Although the integration procedure is reversed, the probability density function of the smallest value $V_1$ can be derived in the same fashion:

$$g(v_1) = n\cdot r(v_1)\{1-R(v_1)\}^{n-1}. \tag{8}$$

The cumulative distribution function of $V_1$ becomes

$$G(v_1) = \{1-R(v_1)\}^n. \tag{9}$$

The modal value of $g(v_n)$, $\overline{V}_n$, is the extreme value most likely to occur in $n$ observations and it satisfies the following equation:

$$\frac{\mathrm{d}}{\mathrm{d}v_n}g(\overline{v}_n) = 0. \tag{10}$$

Then,

$$1 = -\frac{(n-1)\{r(\overline{v}_n)\}^2}{r'(\overline{v}_n)\cdot R(\overline{v}_n)}. \tag{11}$$

By dividing (11) by $1-R(\overline{v}_n)$, we have

$$\frac{1}{1-R(\overline{v}_n)} = -\frac{n-1}{R(\overline{v}_n)}\frac{r(\overline{v}_n)}{1-R(\overline{v}_n)}\frac{r(\overline{v}_n)}{r'(\overline{v}_n)}. \tag{12}$$

Using the L'Hospital rule for large $\overline{v}_n$,

$$\frac{r(\overline{v}_n)}{1-R(\overline{v}_n)} = -\frac{r'(\overline{v}_n)}{r(\overline{v}_n)}. \tag{13}$$

Substituting (13) into (12),

$$\frac{1}{1-R(\overline{v}_n)} = \frac{n-1}{R(\overline{v}_n)} \sim n \quad \text{for large } n \text{ and } \overline{v}_n. \tag{14}$$

Finally,

$$R(\overline{v}_n) \sim 1-\frac{1}{n} \quad \text{for large } n \text{ and } \overline{v}_n. \tag{15}$$

Then,

$$R(\overline{v}_n) = 1-\mathrm{e}^{-\overline{v}_n^2/2\sigma^2} = 1-\frac{1}{n}. \tag{16}$$

Therefore,

$$\overline{v}_n = \sqrt{\ln n}\sqrt{2\sigma^2} = \sigma\sqrt{2\cdot\ln n}. \tag{17}$$

When $v$ is large, the difference between $F(v)$ and $R(v)$ is less than 9% (**Figure 2**), so the value of $\overline{v}_n$ obtained by replacing $R(\overline{v}_n)$ with $F(\overline{v}_n)$ in Equation (15) is approximately equal to that in Equation (17) for large $n$.

Similarly, the modal value of $g(v_1)$, $\overline{V}_1$, is the extreme value most likely to occur in $n$ observations and it satisfies the following equation:

$$\frac{\mathrm{d}}{\mathrm{d}v_1} g(\overline{v}_1) = 0. \tag{18}$$

Then,

$$1 = \frac{(n-1)\{r(\overline{v}_1)\}^2}{r'(\overline{v}_1)\cdot\{1-R(\overline{v}_1)\}}. \tag{19}$$

By dividing (19) by $R(\overline{v}_1)$, we have

$$\frac{1}{R(\overline{v}_1)} = \frac{n-1}{1-R(\overline{v}_1)} \frac{r(\overline{v}_1)}{R(\overline{v}_1)} \frac{r(\overline{v}_1)}{r'(\overline{v}_1)}. \tag{20}$$

Using the L'Hospital rule for small $\overline{v}_1$,

$$\frac{r(\overline{v}_1)}{R(\overline{v}_1)} = \frac{r'(\overline{v}_1)}{r(\overline{v}_1)}. \tag{21}$$

Substituting (21) into (20),

$$\frac{1}{R(\overline{v}_1)} = \frac{n-1}{1-R(\overline{v}_1)} \text{ for large } n \text{ and small } \overline{v}_1. \tag{22}$$

Since $R(\overline{v}_1) \sim 0$ and $n-1 \sim n$ for large $n$ and small $\overline{v}_1$,

$$R(\overline{v}_1) \sim \frac{1}{n}. \tag{23}$$

Then,

$$R(\overline{v}_1) = 1 - \mathrm{e}^{-\overline{v}_1^2/2\sigma^2} = \frac{1}{n}. \tag{24}$$

Therefore,

$$\overline{v}_1 = \sqrt{\ln\left(\frac{n}{n-1}\right)}\sqrt{2\sigma^2} = \sigma\sqrt{2\cdot\ln\left(\frac{n}{n-1}\right)}. \tag{25}$$

When $v$ is small, the difference between $F(v)$ and $R(v)$ is can reach 45% (**Figure 2**); nevertheless, the value of $\overline{v}_1$ obtained by replacing $R(\overline{v}_1)$ with $F(\overline{v}_1)$ in Equation (23) is approximately equal to that in Equation (25) for large $n$.

Finally, the range of $(v_1, v_2, v_3, \cdots, v_n)$ denoted by $R_n$,

$$R_n \equiv \overline{v}_n - \overline{v}_1 = \sqrt{2}\sigma\left(\sqrt{\ln n} - \sqrt{\ln\left(\frac{n}{n-1}\right)}\right). \tag{26}$$

**Figure 3** illustrates how $D_n$ changes with varying $n$. In the NIF experiment, 192 lasers were indirectly directed at the fuel, and the range of the implosion velocity at that time is estimated to be 2.221. In contrast, if only 62 lasers are used, the range of the implosion velocity is expected to be 1.904, representing a 14.3% reduction. Moreover, if only 26 lasers are used, the range of the implosion velocity is expected to be 1.607, representing a 27.6% reduction. As shown in **Figure 4(a)**, it is possible to uniformly irradiate a spherical fuel target using 62 laser devices. In detail, the spherical fuel is modeled as a globe, onto which six great circles passing through the North and South Poles are uniformly arranged. Along each great circle, twelve points including the polar positions are evenly allocated. Consequently, a total of 62 points are uniformly distributed on the spherical surface. Laser irradiation is then applied from 62 devices, each directed toward one of these designated points. In **Figure 4(b)**, it is possible to uniformly irradiate a spherical fuel target using 26 laser devices. Similarly, the spherical fuel is modeled as a globe, onto which four great circles passing through the North and South Poles are uniformly arranged. Along each great circle, eight points including the polar positions are evenly allocated. Consequently, a total of 26 points are uniformly distributed on the spherical surface. Laser irradiation is then applied from 26 devices, each directed toward one of these designated points. By adopting this configuration, the range in implosion velocity can be reduced compared to the NIF experimental setup. Moreover, it would be appropriate to increase the output of each laser device so that the total laser energy exceeds that of the NIF system.

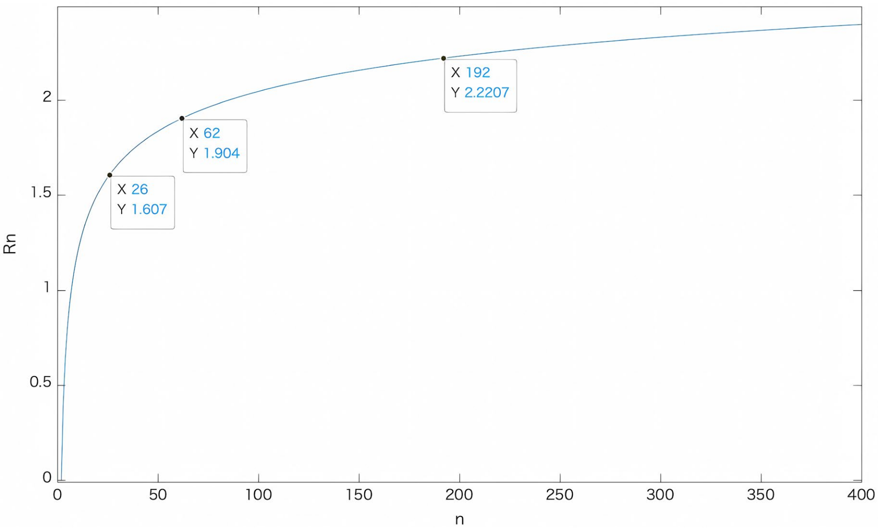


**Figure 3.** Relationship between the number of laser shots $n$ and the range, $R_n$, in implosion velocity resulting from $n$ laser shots. The unit of $R_n$ is the standard deviation, $\sigma$.

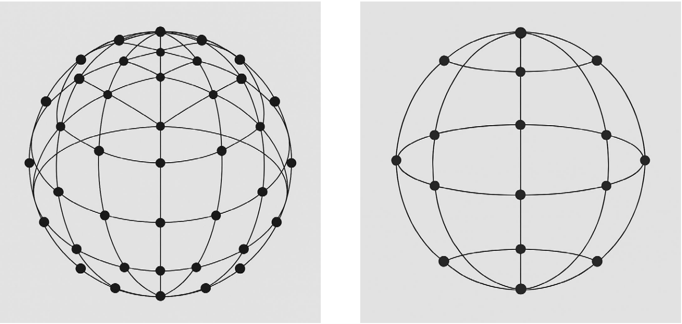

(a) (b)

**Figure 4.** (a) Irradiating the spherical fuel uniformly with 62 lasers; each great circle is irradiated with 12 lasers; (b) Irradiating the spherical fuel uniformly with 26 lasers; each great circle is irradiated with 8 lasers. For clarity in figures (a) and (b), the irradiation points are shown only partially.

## 3. Discussion

In this study, we use extreme value statistics to quantitatively estimate the relationship between the number of laser beams and the range in implosion-related velocity. As a result, while 192 laser beams were used in the NIF experiment, it is found that reducing the number of beams to 62 can decrease the range by 14.3%, and to 26 by 27.6%. A reduction in range increases the likelihood of more effective implosion, thereby enhancing the probability of fuel ignition.

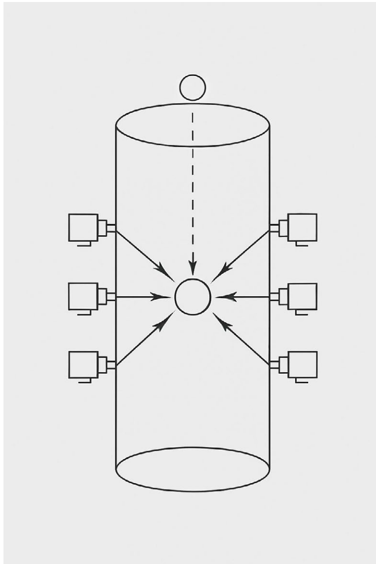

Figure 5. A spherical fuel pellet is dropped in free fall from the top end of a long cylinder. In this figure, only six laser devices are shown for simplicity, but in reality, simultaneous irradiation is performed with 26 laser devices. These 26 devices are treated as one set, and seven such sets are arranged along the cylinder. In each set, the fuel is irradiated simultaneously at the moment it passes through that position.

Reducing the number of laser beams decreases the total energy delivered, making it essential to enhance the output of each individual laser device. However, in addition to increasing output, an alternative approach is to arrange 26 laser units evenly around the circumference of a long cylindrical structure in seven sets. Figure 5 shows a single set of the apparatus. Seven such sets are arranged along the cylinder. Thus, the total number of laser devices in these seven sets would be 182 out of the 192 devices used in the NIF experiment to construct the new irradiation system. A spherical fuel target is then dropped freely from the top, and laser irradiation is timed precisely as it passes through each set. This configuration enables continuous irradiation. While current laser systems require cooling after each shot and cannot operate at extremely short intervals, this method allows for continuous operation. In the current laser system, the thermal radiation generated during implosion is reflected by mirrors to protect the laser devices. However, because the mirrors have insufficient heat resistance and cannot be reused easily, the NIF placed the fuel inside a pot-like device and fired the lasers from outside the pot toward its inner wall. This indirect irradiation allowed only 14.2% (= 270 kJ/1900 kJ) of the lasers' total thermal output to reach the fuel. Therefore, in the system we propose, even without the use of mirrors, the freely falling fuel rapidly moves downward from the point of irradiation, thereby avoiding the impact of thermal radiation on the laser devices. Moreover, if the small windows at the laser output ports are closed instantaneously, the protection would be virtually perfect. Most importantly, the key advantage of the system is that it allows the lasers to be directed at the fuel directly. In the NIF experiment, of the total laser output of 1900 kJ, 270 kJ was indirectly delivered to the fuel pellet, resulting in a generated energy of 1370 kJ. Therefore, it is expected that if 182 of the NIF laser units were rearranged in the manner proposed in this new system to directly irradiate the fuel, an energy of 1801 kJ (= 1900 kJ/192 × 182) would be deposited into the fuel, leading to ignition with higher efficiency. However, the expected drawback of this new system is that it will be challenging to accurately irradiate with a laser when the fuel pellet's trajectory becomes unstable due to laser irradiation. This can be improved to some extent by narrowing the cylinder radius. Another issue, which is not limited to this system, is how to mitigate interference caused by implosion associated with laser irradiation. There are several possible countermeasures, but one approach could involve changing the laser for each set and using multiple frequencies to partially disrupt coherence, thereby reducing the impact of interference.

## 4. Conclusion

This study quantitatively evaluate, using probabilistic methods, the relationship between the total number of laser devices and the range in implosion performance. In particular, it is found that when using 26 laser devices per set, the range is reduced by 27.6% compared with the NIF experiment. By arranging seven such sets along a long cylinder and allowing the fuel to fall freely from the top, sequentially irradiating it as it passes through each set, it should be possible to avoid the current issue of mirror use while enabling direct irradiation. If the current NIF system is modified into the system we propose, it would likely make fuel ignition achievable.

## Conflicts of Interest

The author declares no conflicts of interest regarding the publication of this paper.

## References

[1] Clery, D. (2014) A Piece of the Sun: The Quest for Fusion Theory. MIT Press.

[2] Labaune, C., Baccou, C., Depierreux, S., Goyon, C., Loisel, G., Yahia, V., *et al.* (2013) Fusion Reactions Initiated by Laser-Accelerated Particle Beams in a Laser-Produced Plasma. *Nature Communications*, **4**, Article No. 2506. https://doi.org/10.1038/ncomms3506

[3] Abu-Shawareb, H., Acree, R., Adams, P., Adams, J., Addis, B., Aden, R., *et al.* (2024) Achievement of Target Gain Larger than Unity in an Inertial Fusion Experiment. *Physical Review Letters*, **132**, Article ID: 065102. https://doi.org/10.1103/physrevlett.132.065102

[4] Osaka, M. (2024) Approximating the Radial Distribution Function of the Electron in a Hydrogen Atom by a Normal Distribution Suggests That Magnetic Confinement Fusion Would Be Less Energy Efficient than Inertial Confinement Fusion. *Applied Mathematics*, **15**, 585-593. https://doi.org/10.4236/am.2024.159035

[5] Zylstra, A.B., Hurricane, O.A., Callahan, D.A., Kritcher, A.L., Ralph, J.E., Robey, H.F., *et al*. (2022) Burning Plasma Achieved in Inertial Fusion. *Nature*, **601**, 542-548. https://doi.org/10.1038/s41586-021-04281-w

[6] Ochi, M.K. (1990) Applied Probability & Stochastic Processes. A Wiley-Interscience Publication.

[7] Koning, P. (2024) Enhanced Yield Capability Proposal Aims to Boost NIF Yield. https://lasers.llnl.gov/news/enhanced-yield-capability-proposal-aims-to-boost-nif-yield